

# Synthesis Optimization and Crystal Structures of Layered Metal(IV) Hydrogen Phosphates, $\alpha$ -M(HPO<sub>4</sub>)<sub>2</sub>·H<sub>2</sub>O (M = Ti, Sn, Pb)

Sebastian Bruque,\* Miguel A. G. Aranda, Enrique R. Losilla, Pascual Olivera-Pastor, and Pedro Maireles-Torres

Departamento de Química Inorgánica, Universidad de Málaga, Aptd. 59, 29071 Málaga, Spain

Received July 29, 1994<sup>⊗</sup>

The syntheses of three layered metal(IV) hydrogen phosphates with formula  $\alpha$ -M(HPO<sub>4</sub>)<sub>2</sub>·H<sub>2</sub>O (M = Ti, Sn, Pb) have been optimized to yield single phases of highly crystalline materials. The crystal structures of these compounds have been studied using X-ray powder diffraction data by the Rietveld method. These three hydrogen phosphates are isomorphous and belong to the  $\alpha$ -Zr(HPO<sub>4</sub>)<sub>2</sub>·H<sub>2</sub>O structure type. The unit cell parameters are as follows: M = Ti,  $a = 8.6403(2)$  Å,  $b = 5.0093(1)$  Å,  $c = 15.5097(4)$  Å,  $\beta = 101.324(2)^\circ$ , space group  $P2_1/n$ ; M = Sn,  $a = 8.6115(3)$  Å,  $b = 4.9643(5)$  Å,  $c = 15.861(2)$  Å,  $\beta = 100.003(1)^\circ$ , space group  $C2/c$ ; M = Pb,  $a = 8.6238(4)$  Å,  $b = 4.9870(2)$  Å,  $c = 16.1250(6)$  Å,  $\beta = 100.615(3)^\circ$ , space group  $P2_1/n$ . The agreement factors obtained by Rietveld refinements,  $R_{wp}$ , ranged between 12.5 and 9%. Although the prototype of this series is  $\alpha$ -ZrP, here we report that the volume of the unit cell of this compound is markedly larger than the volumes of the other studied members of the series. This is due to the presence of less corrugated layers in  $\alpha$ -ZrP. IR and thermal studies of M(HPO<sub>4</sub>)<sub>2</sub>·H<sub>2</sub>O (M = Ti, Sn, Zr, Pb) indicate the existence of a trend in the strength of the H-bonds that retain the hydration water in the interlayer region.

## Introduction

Layered hydrogen phosphates of metals in oxidation state IV of composition M(HPO<sub>4</sub>)<sub>2</sub>·H<sub>2</sub>O (M = Si, Ge, Sn, Pb, Ti, Zr, Hf) constitute an isostructural series and thereafter will be referred as  $\alpha$ -MP. Precise structural data have been derived only for M = Zr.<sup>1–3</sup> Other structural studies have shown that for M = Ti<sup>4</sup> and Hf<sup>5</sup> the frameworks are similar to that of analogous zirconium although the precision of the reported data is quite low, probably due to the low degree of crystallinity of the synthesized products.

In a first single crystal study, Clearfield and Smith<sup>1</sup> described the framework of Zr(HPO<sub>4</sub>)<sub>2</sub>·H<sub>2</sub>O in the  $P2_1/c$  space group. In a later work, a monoclinic unit cell with a smaller  $\beta$  angle was chosen,<sup>2</sup> resulting in the  $P2_1/n$  space group. The positions of the hydrogen atoms were determined by Albertsson et al.<sup>3</sup> using neutron powder diffraction, although the sample was not deuterated. The structure (Figure 1) of  $\alpha$ -ZrP is built up of layers of slightly distorted ZrO<sub>6</sub> octahedra and alternating (up and down) HPO<sub>4</sub> tetrahedra. These layers have a pseudo-hexagonal symmetry (see Figure 2) and are stacking along the  $c$ -axis. The water molecules are located in the interlayer space and participate in the hydrogen-bond network. The oxygen of the water acts as donor in one H-bond with the oxygen of a neighboring POH group. The other water hydrogen does not participate in H-bonding. Both acidic POH groups in the same layer form hydrogen bonds with the oxygen of the water molecule. The layers are only bound by van der Waals forces.

These materials have been extensively studied as ionic exchangers,<sup>6</sup> acid solids,<sup>7</sup> hosts in intercalation reactions,<sup>8,9</sup>

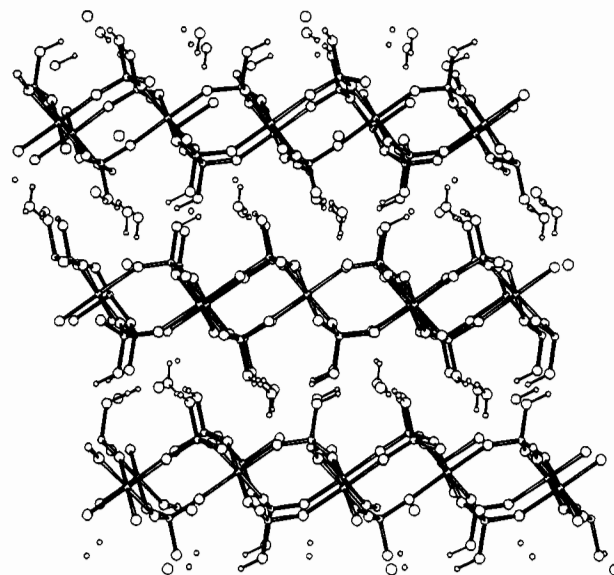


Figure 1. ORTEP view along the  $b$ -axis ( $c$ -axis vertical) of the crystal structure of  $\alpha$ -Zr(HPO<sub>4</sub>)<sub>2</sub>·H<sub>2</sub>O.

sensors,<sup>10</sup> etc. As exemplified for  $\alpha$ -ZrP,<sup>11</sup> the chemical reactivity and hydrolytic stability of this phosphate vary with the degree of crystallinity. Thus, the synthetic method plays a key role in determining the structural parameters and reactivity of the resulting sample.

It is not possible to establish a unique method for the synthesis of all the  $\alpha$ -MP. This is due to the fact that the starting materials

<sup>⊗</sup> Abstract published in *Advance ACS Abstracts*, January 1, 1995.

- (1) Clearfield, A.; Smith, G. D. *Inorg. Chem.* **1969**, *8*, 431.
- (2) Troup, J. M.; Clearfield, A. *Inorg. Chem.* **1977**, *16*, 3311.
- (3) Albertsson, J.; Oskarsson, A.; Tellgren, R.; Thomas, J. O. *J. Phys. Chem.* **1977**, *81*, 1774.
- (4) Christensen, A. N.; Andersen, E. K.; Andersen, I. G. K.; Alberti, G.; Nielsen, M.; Lehmann, M. S. *Acta Chem. Scand.* **1990**, *44*, 865.
- (5) Nakai, I.; Imai, K.; Kawashima, T.; Ohsumi, K.; Izumi, F.; Tomita, I. *Anal. Sci.* **1990**, *6*, 689.

(6) Clearfield, A. In *Inorganic Ion Exchange Materials*; CRC Press: Boca Raton, FL, 1982.

(7) Hattori, T.; Ishiguro, A.; Murakami, Y. *J. Inorg. Nucl. Chem.* **1978**, *40*, 1107.

(8) Alberti, G. In *Recent Developments in Ion Exchange*; Williams, P. A., Hudson, M. J., Eds.; Elsevier Applied Science: New York, 1987.

(9) Rodriguez-Castellon, E.; Rodriguez, A.; Bruque, S. *Inorg. Chem.* **1984**, *24*, 1187.

(10) Alberti, G. *Pontif. Acad. Sci.* **1976**, *40*, 629.

(11) Clearfield, A. *Comments Inorg. Chem.* **1990**, *10*, 89.

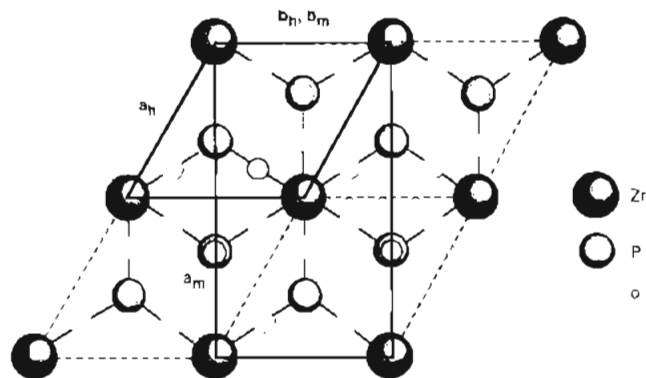


Figure 2. Idealized view of one layer of  $\alpha$ -Zr(HPO<sub>4</sub>)<sub>2</sub>·H<sub>2</sub>O showing the relationship between the pseudo-hexagonal cell and the real monoclinic unit cell.

are very different and the nature of the reaction media influences the hydrolytic stability of the products. Each synthesis requires its own optimum conditions to yield the desired material. Some structural studies have obtained poor results because the sample was poorly crystalline or a mixture of phases or both. For example, the powder diffraction patterns for  $\alpha$ -TiP and  $\gamma$ -TiP<sup>4</sup> contains extra diffraction peaks, which clearly indicates more than one phase, and for the  $\alpha$ -phase the peaks were quite broad showing low crystallinity. These two features led to very poor results for the structure of  $\alpha$ -TiP. So far, there are no published studies about the crystal structures of  $\alpha$ -SnP and  $\alpha$ -PbP. This is probably due to the low degree of crystallinity of the first compound, when it is synthesized by the conventional methods, and to the low hydrolytic stability of the second compound.

In this work we have optimized the synthesis of  $\alpha$ -TiP,  $\alpha$ -SnP, and  $\alpha$ -PbP. The compounds are found in highly crystalline single phases. We have also studied their crystal structures using X-ray powder diffraction data. We will compare the results with those of the main member of the series  $\alpha$ -ZrP.

### Experimental Section

**Ti(HPO<sub>4</sub>)<sub>2</sub>·H<sub>2</sub>O.**  $\alpha$ -TiP was obtained from "active" titanium dioxide (Eurotitanium from Tioxide, batch 1143, which is mainly anatase with a high surface,  $S_0 = 60 \text{ m}^2/\text{g}$ ) and phosphoric acid. A typical procedure is described: 2 g of "Tioxide" was refluxed overnight with 50 mL of H<sub>3</sub>PO<sub>4</sub> (85% w/w). Then, 30 mL of water was added and the mixture was refluxed for three days more. The resulting solid was filtered off and washed with deionized water several times, and finally with acetone. For the preparation of Ti(DPO<sub>4</sub>)<sub>2</sub>·D<sub>2</sub>O, D<sub>3</sub>PO<sub>4</sub> and D<sub>2</sub>O were used. Unfortunately, during the reflux some H<sub>2</sub>O from the atmosphere was introduced yielding a product only partially deuterated.

**Sn(HPO<sub>4</sub>)<sub>2</sub>·H<sub>2</sub>O.**  $\alpha$ -SnP was synthesized under hydrothermal conditions. Typically, 3 g of SnCl<sub>4</sub>·5H<sub>2</sub>O was added to 20 mL of phosphoric acid (85%). The reaction was carried out in a Berghof autoclave with autogenous pressure at 150 °C for 7 days. The sample was constantly stirred by using magnetic stirring at  $\approx 700 \text{ m}^{-1}$ . The obtained solid was filtered off, washed with deionized water until the pH of the washing liquids was  $\approx 4$ , and dried in a desiccator over P<sub>2</sub>O<sub>5</sub>.

**Zr(HPO<sub>4</sub>)<sub>2</sub>·H<sub>2</sub>O.**  $\alpha$ -ZrP was prepared by the standard fluoro complex method,<sup>12</sup> which yields the highest crystalline material.

**Pb(HPO<sub>4</sub>)<sub>2</sub>·H<sub>2</sub>O.** The preparation method of  $\alpha$ -PbP has been optimized after studying the influence of different parameters as concentration, addition order of the reactants, refluxing time, washing agents, etc.  $\alpha$ -PbP was obtained by reaction of orthophosphoric acid and lead tetraacetate. Pb(CH<sub>3</sub>COO)<sub>4</sub> has to be purified by recrystallization prior to use, until colorless needles have been obtained. The presence of Pb(II) autocatalyzes the reduction of Pb(IV), and the actions of reductor agents have to be avoided. Water hydrolyzes the tetraacetate resulting in unreactive PbO<sub>2</sub>, which implies that the reaction vessels

Table 1. Details of the X-ray Powder Diffraction Patterns for  $\alpha$ -M(HPO<sub>4</sub>)<sub>2</sub>·H<sub>2</sub>O

	$\alpha$ -TiP	$\alpha$ -SnP	$\alpha$ -ZrP	$\alpha$ -PbP
2 $\Theta$ /deg	15	15	15	15
2 $\Theta$ /deg	110	85	75	100
step size/deg	0.02	0.02	0.02	0.03
counting time/s	18	20	15	15

have to be dried previously. A typical procedure is given: 1.5 g of Pb(CH<sub>3</sub>COO)<sub>4</sub> is dissolved in 17 mL of hot glacial acetic acid in a round-bottom flask. Then 20 mL of H<sub>3</sub>PO<sub>4</sub> (85% w/w) and 12 mL of H<sub>2</sub>O were added (in this sequence). The white suspension is gently refluxed for 48 h, and then 1–2 mL of concentrated nitric acid was added by the flask wall. Refluxing was continued for 48 h more. The white solid was filtered off on a sintered disk filter funnel and washed twice with nitric acid (0.2 M), two times with deionized water, and two more times with acetone free of reducing agents.

X-ray diffraction patterns were recorded on a Siemens D501 automated diffractometer using graphite-monochromated Cu K $\alpha$  radiation. The data were collected in the Bragg–Brentano ( $\theta/2\theta$ ) geometry (reflection mode). The experimental conditions used for each pattern are given in Table 1. The data were transferred to a VAX 8530 computer for Rietveld analysis<sup>13</sup> by the GSAS program<sup>14</sup> using a pseudo-Voigt peak shape function corrected for asymmetry at low angles and a refined background function. The first peak at approximately 8 Å was not used in any refinement as the strong asymmetry leads to severe problems for the description of the peak shape.

The water contents were obtained from the combined thermogravimetric (TGA) and differential (DTA) thermal analysis. These studies were carried out in air on a Rigaku Thermoflex apparatus at a heating rate of 10 K/min with calcined Al<sub>2</sub>O<sub>3</sub> as standard. Infrared spectra were recorded on a Perkin-Elmer 883 spectrometer using a dry KBr pellet containing 2% of the sample.

### Results

**Ti(HPO<sub>4</sub>)<sub>2</sub>·H<sub>2</sub>O.** The X-ray powder diffraction pattern of  $\alpha$ -TiP was autoindexed using the programs TREOR<sup>15</sup> and LATTPARM.<sup>16</sup> Both programs gave the same values for the parameters of the unit cell. As an example we report the result of the TREOR program:  $a = 8.637 \text{ \AA}$ ,  $b = 5.009 \text{ \AA}$ ,  $c = 15.499 \text{ \AA}$ , and  $\beta = 101.26^\circ$ . The figures of merit were  $M_{20} = 22$ <sup>17</sup> and  $F_{20} = 31$ <sup>18</sup> (0.006, 106). This cell is very similar to that early reported<sup>19</sup> and related to that of  $\alpha$ -ZrP (space group  $P2_1/n$ ,  $a = 9.060 \text{ \AA}$ ,  $b = 5.297 \text{ \AA}$ ,  $c = 15.414 \text{ \AA}$ , and  $\beta = 101.71^\circ$ ),<sup>2</sup> so we attempted to fit the X-ray profile of  $\alpha$ -TiP using the crystal structure of  $\alpha$ -ZrP as the starting model in the  $P2_1/n$  space group. First, we refined the overall parameters (background, histogram scale factor, zero shift error, unit cell parameters, and peak shape parameters for the pseudo-Voigt function). In a second stage, we refine the atomic parameters (position) and later the temperature factors. Due to the complexity of the structure and the limited resolution of our data we had problems in our refinements (some negative temperature factors were obtained). To overcome this problem we have constrained all temperature factors of a type of atom to have the same value. The final refinement converged to  $R_{wp} = 9.2\%$ ,  $R_p = 6.5\%$  and  $R_f = 3.8\%$ . The refined unit cell

(13) Rietveld, H. M. *J. Appl. Crystallogr.* **1969**, *2*, 65.

(14) Larson, A. C.; Von Dreele, R. B. Los Alamos National Laboratory Report No. LA-UR-86-748, 1987.

(15) Werner, P. E. *Z. Kristallogr.* **1969**, *120*, 375. Werner, P. E.; Eriksson, L.; Westdahl, M. *J. Appl. Crystallogr.* **1985**, *18*, 367.

(16) Garvey, R. LATTPARM autoindexing program" Department of Chemistry, North Dakota State University, Fargo, ND 58105-5516. See also: Garvey, R. *Powder Diffr.* **1986**, *1*, 114.

(17) Wolff, P. M. d. *J. Appl. Crystallogr.* **1968**, *1*, 108.

(18) Smith, G. S.; Snyder, R. L. *J. Appl. Crystallogr.* **1979**, *12*, 60.

(19) Clearfield, A. In *Ion Exchange and Solvent Extraction*; Marinsky, J. A., Marcus, Y., Eds.; Dekker: New York, 1973; Vol. V, Chapter 1.

(12) Alberti, G.; Torracca, E. *J. Inorg. Nucl. Chem.* **1968**, *30*, 317.

**Table 2.** Some Crystal Chemistry Parameters for  $\alpha$ -M(HPO<sub>4</sub>)<sub>2</sub>·H<sub>2</sub>O

	$\alpha$ -TiP	$\alpha$ -SnP	$\alpha$ -ZrP	$\alpha$ -PbP
IR <sup>a</sup> /Å	0.61	0.69	0.72	0.78
a <sub>m</sub> /Å	8.6403(2)	8.6115(3)	9.0664(3)	8.6238(4)
b <sub>m</sub> /Å	5.0093(1)	4.9643(5)	5.2935(2)	4.9870(2)
c <sub>m</sub> /Å	15.5097(4)	15.8605(16)	15.4465(4)	16.1250(6)
$\beta$ /deg	101.324(2)	100.03(1)	101.694(2)	100.615(3)
V/Å <sup>3</sup>	658.22(4)	667.6(1)	725.94(5)	681.62(5)
(area/poh)/Å <sup>2</sup>	21.64	21.38	24.00	21.50
a <sub>h</sub> <sup>b</sup> /Å	4.988	4.972	5.234	4.979
b <sub>h</sub> <sup>b</sup> /Å	5.009	4.964	5.294	4.987
c <sub>h</sub> <sup>b</sup> /Å	22.812	23.43	22.689	23.77
M—O(1)/Å	1.992(7)	1.863(11) (×2)	2.048(2) <sup>c</sup>	1.954(15)
M—O(2)/Å	1.918(8)	2.196(15) (×2)	2.074(2) <sup>c</sup>	1.996(22)
M—O(3)/Å	1.967(9)	2.023(15) (×2)	2.071(2) <sup>c</sup>	2.097(20)
M—O(5)/Å	1.845(8)		2.054(2) <sup>c</sup>	2.310(21)
M—O(6)/Å	2.026(8)		2.065(2) <sup>c</sup>	2.149(22)
M—O(7)/Å	1.926(7)		2.075(2) <sup>c</sup>	2.171(22)
⟨M—O⟩/Å	1.95	2.03	2.06	2.11

<sup>a</sup> Shannon ionic radius for the tetravalent cations in an octahedral environment.<sup>17</sup> <sup>b</sup> Dimensions of the pseudohexagonal unit cell: a<sub>h</sub> = a<sub>m</sub>/2 cos 30; b<sub>h</sub> = b<sub>m</sub>; c<sub>h</sub> = 1.5 c<sub>m</sub> cos(β - 90). <sup>c</sup> Values taken from ref 2.

**Table 3.** Atomic Parameters for  $\alpha$ -Ti(HPO<sub>4</sub>)<sub>2</sub>·H<sub>2</sub>O in Space Group P2<sub>1</sub>/n

atom	x	y	z	B (Å <sup>2</sup> )
Ti	0.2464(2)	0.2544(9)	0.4880(1)	0.59(4)
P(1)	0.3891(4)	0.7447(12)	0.3905(2)	0.18(4)
P(2)	-0.1335(4)	0.2424(12)	0.4027(2)	0.18(-)
O(1)	0.5449(8)	0.8347(16)	0.4376(5)	0.35(4)
O(2)	0.3387(9)	0.4836(17)	0.4128(5)	0.35(-)
O(3)	0.2717(9)	0.9362(18)	0.4176(5)	0.35(-)
O(4)	0.3832(7)	0.7793(19)	0.2919(4)	0.35(-)
O(5)	-0.2363(9)	0.4452(16)	0.4446(5)	0.35(-)
O(6)	-0.1436(9)	-0.0478(17)	0.4260(5)	0.35(-)
O(7)	0.0439(8)	0.3302(16)	0.4148(4)	0.35(-)
O(8)	-0.1958(6)	0.2235(20)	0.3000(4)	0.35(-)
O(9)	0.0040(7)	0.7527(18)	0.2667(4)	0.35(-)

**Table 4.** Atomic Parameters for  $\alpha$ -Sn(HPO<sub>4</sub>)<sub>2</sub>·H<sub>2</sub>O in Space Group C2/c

atom	x	y	z	B (Å <sup>2</sup> )
Sn	0.25	0.25	0.50	1.02(6)
P	0.3776(12)	0.758(3)	0.3939(3)	1.1(1)
O(1)	0.552(1)	0.757(4)	0.431(1)	1.1(2)
O(2)	0.371(2)	0.453(2)	0.407(1)	1.1(-)
O(3)	0.254(2)	0.893(3)	0.439(1)	1.1(-)
O(4)	0.364(3)	0.806(3)	0.298(1)	1.1(-)
O(5)	0.00	0.764(8)	0.25	1.1(-)

**Table 5.** Atomic Parameters for  $\alpha$ -Pb(HPO<sub>4</sub>)<sub>2</sub>·H<sub>2</sub>O in Space Group P2<sub>1</sub>/n

atom	x	y	z	B (Å <sup>2</sup> )
Pb	0.2470(3)	0.2546(9)	0.4897(1)	0.13(4)
P(1)	0.384(2)	0.745(3)	0.3855(6)	0.2(2)
P(2)	-0.127(2)	0.217(3)	0.3981(6)	0.2(-)
O(1)	0.555(2)	0.683(6)	0.432(1)	0.0(2)
O(2)	0.335(3)	0.429(3)	0.397(2)	0.0(-)
O(3)	0.268(3)	0.905(5)	0.420(2)	0.0(-)
O(4)	0.375(3)	0.786(6)	0.291(1)	0.0(-)
O(5)	-0.262(2)	0.347(5)	0.436(1)	0.0(-)
O(6)	-0.101(3)	-0.074(4)	0.431(2)	0.0(-)
O(7)	0.024(2)	0.389(5)	0.417(1)	0.0(-)
O(8)	-0.179(3)	0.203(6)	0.300(1)	0.0(-)
O(9)	-0.009(4)	0.777(8)	0.263(1)	0.0(-)

parameters and metal—oxygen bond distances are given in Table 2. Results of the refinement are given in Table 3, and the final observed, calculated, and difference profiles are shown in Figure 3.

We have also carried out a neutron powder diffraction study at the D1A diffractometer (Saclay nuclear reactor, Paris,

France). Because of problems with the sample (it was not very crystalline due to decreasing of reaction time and only partially deuterated), the results have been poor. In any case, the crystal structure refined from X-ray powder diffraction fits the neutron data and a difference Fourier map revealed two peaks. The peaks centered at (0.43, 0.40, 0.23) and (0.46, 0.25, 0.17) are situated at 0.91 and 0.99 Å from the oxygen of the water molecule, respectively. These positions are quite close to those reported for  $\alpha$ -ZrP,<sup>3</sup> H(3) (0.455, 0.375, 0.266) and H(4) (0.468, 0.273, 0.182). Hence, we can confirm that the hydrogen atoms positions of the water molecule in  $\alpha$ -TiP are very similar to those in  $\alpha$ -ZrP. Unfortunately, we could not obtain the position of the hydrogen atoms of the phosphate groups.

**Sn(HPO<sub>4</sub>)<sub>2</sub>·H<sub>2</sub>O.** The X-ray powder diffraction pattern of  $\alpha$ -SnP is shown in Figure 4. As can be seen, the powder pattern presents slightly broad peaks, which made the autoindexing process difficult. Knowing that this compound is isomorphous to  $\alpha$ -ZrP and  $\alpha$ -TiP, we used the indexes of the first peaks to generate an approximated unit cell and then we refined it by using the CELLREF program, a unit-cell least-square refinement program. The result was a = 8.613 Å, b = 4.970 Å, c = 15.866 Å, and β = 100.05° parameters that are quite similar to those reported by Costantino and Gasperoni.<sup>20</sup> In Figure 4 are also shown the reflection marks allowed for the primitive space group P2<sub>1</sub>/n, and its isomorphic C-centered supergroup C2/c. As the intensity of the primitive peaks are extremely weak (most of the primitive peaks are not observed), we have refined the crystal structure of  $\alpha$ -SnP in the C2/c space group using the structure of  $\alpha$ -ZrP as the starting model but adapting the atomic parameters to the new space group. As it can be observed in Figure 2, the layers of  $\alpha$ -ZrP are pseudo-C-centered, so we only need to modify the atomic parameters slightly.

To refine the crystal structure of  $\alpha$ -SnP we followed the same procedure as that in the  $\alpha$ -TiP case. The peak shape was described using a pseudo-Voigt function. After refinement of the overall parameters, the peak shape was not satisfactorily described. A close inspection of the pattern showed that the (hk0) peaks were sharper than the (hkl) peaks with l ≠ 0. This is a clear evidence of anisotropic peak broadening (along the c axis), which can be modeled inside GSAS.<sup>12</sup> The refinement was better when we used a Lorentzian Scherrer broadening including the anisotropic broadening coefficient. We have used soft constraints in the P—O bond distances, to keep a reasonable PO<sub>4</sub> tetrahedra, with the P—O distances 1.53(2) Å. The final refinement converged to R<sub>wp</sub> = 12.6%, R<sub>p</sub> = 9.6%, and R<sub>F</sub> = 4.9%. The refined unit cell parameters and metal—oxygen bond distances are given in Table 2. Results of the refinement are given in Table 4, and the final observed, calculated, and difference profiles are shown in Figure 4.

**Zr(HPO<sub>4</sub>)<sub>2</sub>·H<sub>2</sub>O.** We have refined the crystal structure of  $\alpha$ -ZrP using X-ray powder diffraction data for the sake of comparison with the other refinements. We used as the starting model the crystal structure reported by Troup and Clearfield using X-ray single crystal data.<sup>2</sup> As we cannot improve the structure, the results are not reported here, but they have been useful to test the refinement procedure and to determine the limits of our study. The refined unit cell parameters are given in Table 2, and the final observed, calculated, and difference profiles are shown in Figure 5.

**Pb(HPO<sub>4</sub>)<sub>2</sub>·H<sub>2</sub>O.** The X-ray powder diffraction pattern of  $\alpha$ -PbP was autoindexed using the program TREOR. The values of the unit cell parameters were a = 8.619 Å, b = 4.983 Å, c = 16.099 Å, and β = 100.24°. The figure of merit were M<sub>17</sub> = 16 and F<sub>17</sub> = 20 (0.008, 115). For the Rietveld refinement

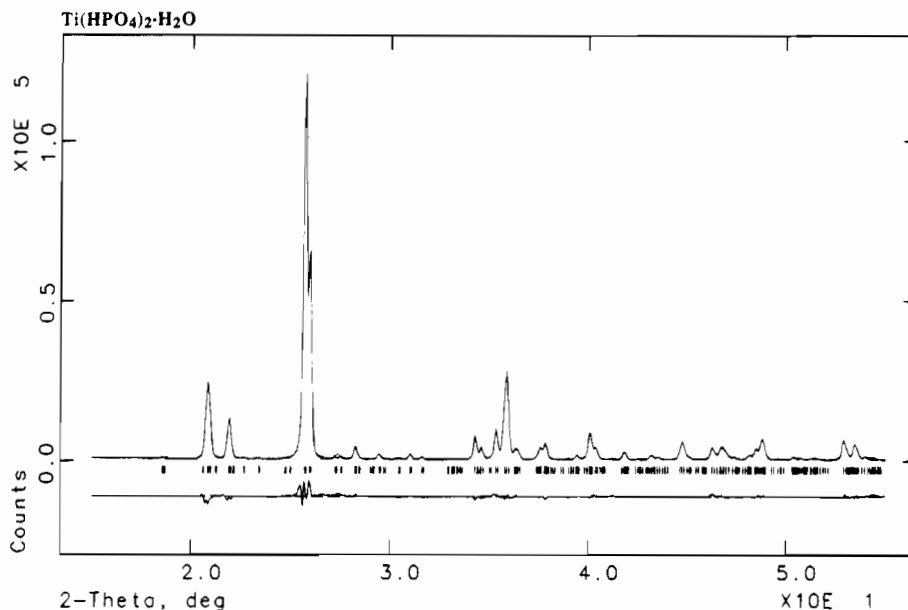


**Figure 3.** Final observed (points), calculated (full line), and difference X-ray profiles for  $\alpha$ - $\text{Ti}(\text{HPO}_4)_2 \cdot \text{H}_2\text{O}$ . Reflection marks are shown for the  $P2_1/n$  space group.

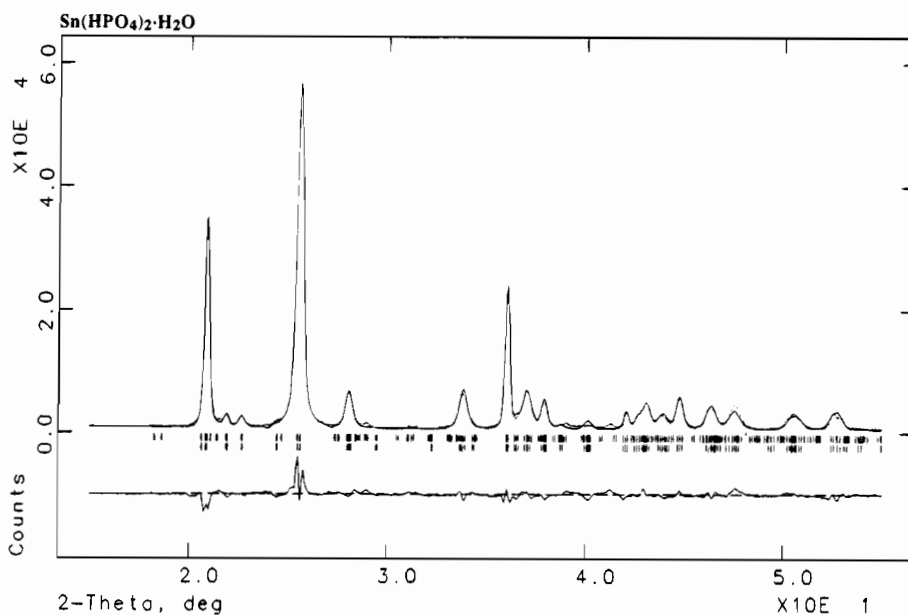


**Figure 4.** Rietveld plot for  $\alpha$ - $\text{Sn}(\text{HPO}_4)_2 \cdot \text{H}_2\text{O}$  as in Figure 3. Reflection marks are shown for the  $P2_1/n$  (up) and  $C2/c$  (down) space groups.

we have followed the same procedure described above. In this refinement we have also used soft constraints in the  $\text{PO}_4$  tetrahedra. The final refinement converged to  $R_{\text{WP}} = 9.9\%$ ,  $R_{\text{P}} = 7.3\%$ , and  $R_{\text{F}} = 3.9\%$ . The refined unit cell parameters and metal–oxygen bond distances are given in Table 2. Results of the refinement are given in Table 5, and the final observed, calculated, and difference profiles are shown in Figure 6.

**IR and Thermal Study.** The hydration water of these layered phosphates has been studied by IR spectroscopy and thermal analysis. As an example, the IR spectrum of  $\alpha$ -PbP is shown in Figure 7. Three characteristic bands are present in the OH stretching region for all members of the series. The two narrow bands above  $3400 \text{ cm}^{-1}$  have been assigned to the asymmetric and symmetric stretching vibrations of the O–H group of the water molecule not interacting by H-bond through the H. This H is directed toward the free cavities, and thus, it is free of any H-bonds. The broad band about  $3000 \text{ cm}^{-1}$  is attributed to the O–H stretching of the other groups that interact by H-bond through the H (i.e. the two POH groups and the

other OH group of the water molecule). Although the H positions are only known for  $\alpha$ -ZrP, our preliminary neutron diffraction study for  $\alpha$ -TiP indicates that the hydrogen positions of the water molecule are very close to those reported for  $\alpha$ -ZrP, with one hydrogen directed toward the zeolitic cavities. Hence, we can assume that this hydrogen is present in all members of the series, in agreement with the IR results. In Table 6 are shown the positions of the two narrow bands for the four studied compounds. The TGA-DTA curves for  $\alpha$ -PbP are shown in Figure 8. The results are in full agreement with those early reported<sup>21</sup> and, hence, are not discussed in this work. The water molecule is lost at ca.  $200^\circ\text{C}$ . In Table 6 are also shown the values of temperatures of the endotherms due to the hydration water release of all members of the studied series.

#### Discussion

To ensure success in a structural study by the Rietveld method, it is very important to have products as a highly crystalline single

(21) Frydrych, R.; Lohoff, K. *Chem. Ber.* **1969**, 4070.

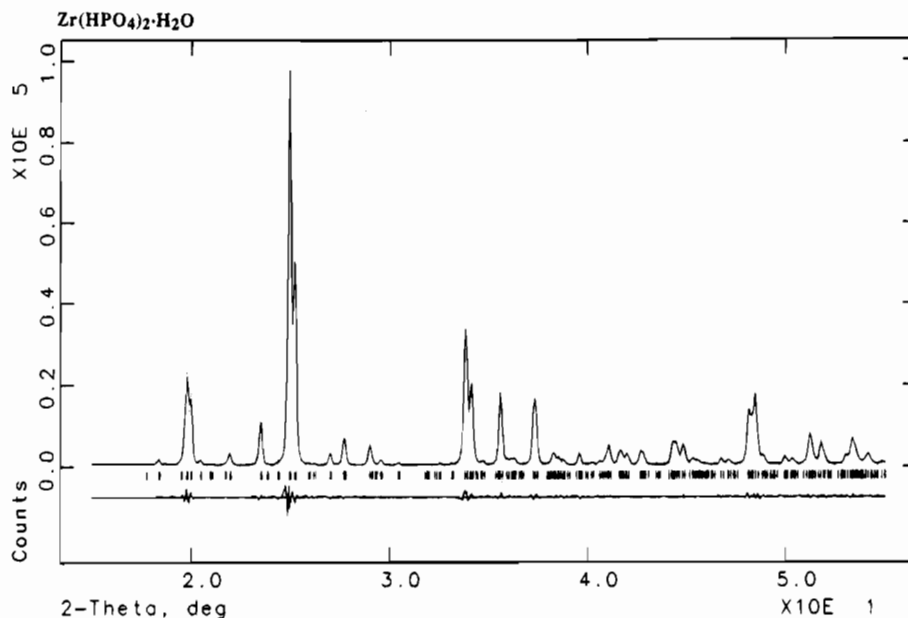


Figure 5. Rietveld plot for  $\alpha$ -Zr(HPO<sub>4</sub>)<sub>2</sub>·H<sub>2</sub>O as in Figure 3.

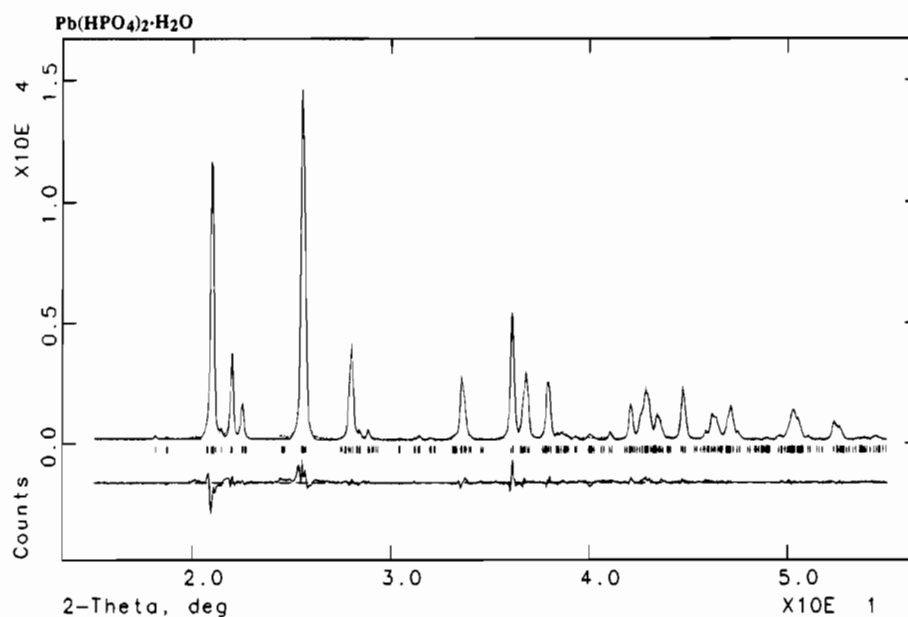


Figure 6. Rietveld plot for  $\alpha$ -Pb(HPO<sub>4</sub>)<sub>2</sub>·H<sub>2</sub>O as in Figure 3.

phase. In the  $\alpha$ -ZrP case, the fluoro complex method has been revealed as the best method to obtain the desired material. But this is not a good method for Ti, Sn, and Pb as the fluoro complexes are not formed or they have very low stability.

On the other hand, long reflux time and high temperature (hydrothermal synthesis) result in higher crystallinity. But in the  $\alpha$ -PbP case, this conditions leads to the reduction of Pb(IV) to Pb(II). It is also very important to optimize the P/Pb ratio and to avoid the presence of Pb(II). The reflux time cannot be very long. For  $\alpha$ -TiP, a very high concentration of H<sub>3</sub>PO<sub>4</sub> may lead to the formation of  $\gamma$ - and  $\beta$ -TiP phases.<sup>22,23</sup> Hence, an initial high concentration of H<sub>3</sub>PO<sub>4</sub> has been used for a short time to allow a fast attack on the reactive TiO<sub>2</sub>, and later the crystallinity is improved by diluting the reaction mixture with water and maintaining the reflux for a long period of time. To obtain  $\alpha$ -SnP, hydrothermal synthesis was employed, instead

of the reflux method.<sup>20</sup> In this later method nitric acid was added, but we have shown that this reactant is not necessary to improve the crystallinity of  $\alpha$ -SnP.

It is important to point out that although the precision of our refinements is much better than that of previous work,<sup>4,5</sup> it is still not very high. In addition to the main drawback of the X-ray powder diffraction technique (the severe overlapping of peaks at high angles) we can underline three factors in our particular case that explain the precision obtained in the determined crystal structures. The first is the complexity of the structure type, 12 non-hydrogen atoms in the asymmetric unit cell, none of them in special positions. Second, the presence of heavy atoms as Pb and Sn also limits the precision in the atomic parameters of the light atoms such as oxygen. A third factor is the broadening of the powder diffraction peaks, although this factor should affect only the  $\alpha$ -SnP case.

On the other hand, the precision in the unit cell edges and angles is high as the synthesized compounds are quite crystalline. In Figure 9 is shown the plot of the unit cell volume versus

(22) Koboyashi, E. *Bull. Chem. Soc. Jpn.* **1975**, *48*, 3314.

(23) Albery, G.; Constantino, U.; Giovagnotti, M. L. *J. Inorg. Nucl. Chem.* **1979**, *41*, 643.

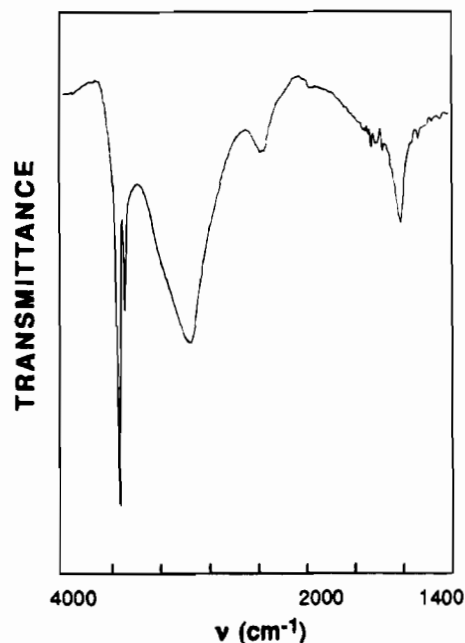


Figure 7. IR spectrum for  $\alpha$ -Pb(HPO<sub>4</sub>)<sub>2</sub>·H<sub>2</sub>O in the 4000–1400 cm<sup>-1</sup> region.

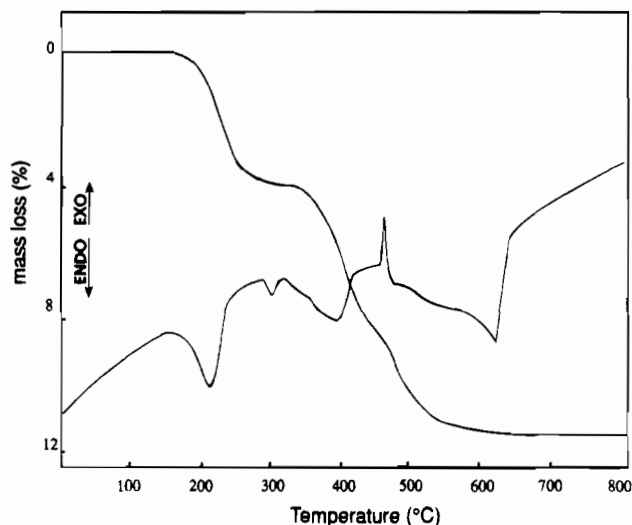


Figure 8. TGA–DTA curves for  $\alpha$ -Pb(HPO<sub>4</sub>)<sub>2</sub>·H<sub>2</sub>O: TGA (up, left) and DTA (down, left).

Table 6. Data for the Hydration Water in  $\alpha$ -M(HPO<sub>4</sub>)<sub>2</sub>·H<sub>2</sub>O (M = Pb, Ti, Sn, Zr)

	$\alpha$ -PbP	$\alpha$ -TiP	$\alpha$ -SnP	$\alpha$ -ZrP
$\nu_{as}(\text{OH})(\text{free})/\text{cm}^{-1}$	3525	3560	3565	3590
$\nu_s(\text{OH})(\text{free})/\text{cm}^{-1}$	3470	3480	3495	3510
temp water loss/°C	200	170	145	135

the Shannon ionic radius<sup>24</sup> for the  $\alpha$ -M(HPO<sub>4</sub>)<sub>2</sub>·H<sub>2</sub>O (M = Ti, Sn, Zr, Pb) series. Clearly, the unit cell volume of  $\alpha$ -ZrP is bigger than those of the other members of the series. As it is shown in Table 2, the increase in the volume is not isotropic. The *a* and *b* unit cell parameters are longer, 9.07 and 5.29 Å, respectively, than those expected (8.60 and 5.00 Å, respectively). The *c* parameter is shorter (15.45 Å instead of 16.05 Å). In other words, the structure of  $\alpha$ -ZrP presents an expansion in the *ab* plane and a small contraction along the *c* axis.

Our structural study indicates that the metal–oxygen bond distances (see Table 2) vary as should be expected from the

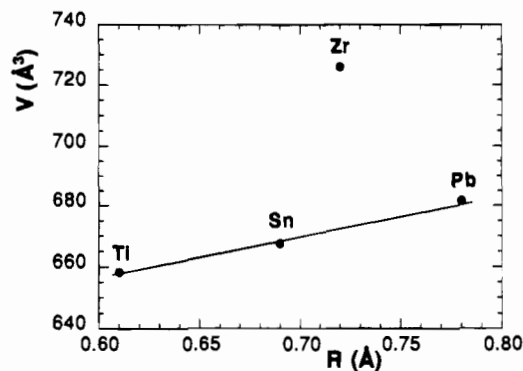


Figure 9. Unit cell volume versus Shannon metal ionic radius plot for the  $\alpha$ -M(HPO<sub>4</sub>)<sub>2</sub>·H<sub>2</sub>O (M = Ti, Sn, Zr, Pb) series.

metal ionic radii (i.e. the Zr–O bond distances are not longer than the Pb–O ones). However the metal phosphorus calculated distances show this anomaly. The reason for this behavior is the position of the metal atoms relative to the central plane. The Zr atoms are displaced  $\pm 0.23$  Å from the plane, Ti atoms are displaced  $\pm 0.19$  Å, Sn is in the plane (due to the space group used, *C2/c*), and Pb is displaced  $\pm 0.17$  Å. Thus, the metal–oxygen–phosphorus angles decrease in the order  $\alpha$ -ZrP >  $\alpha$ -TiP >  $\alpha$ -SnP >  $\alpha$ -PbP, the average angles M–O–P being 150, 145, 142, and 135°, respectively. This has the effect of pulling the metal atoms closer together and, thus, pushing the phosphate groups further into the interlayer space. The more open Zr–O–P angle is responsible for the expansion along the *ab* plane and the slight contraction along the *c* axis. As a consequence, the layers of  $\alpha$ -ZrP are slightly thinner (along the *c* axis) but more extended in the *ab* plane than those for M = Ti, Sn, and Pb. In these last compounds the corrugation of the layers is more pronounced than in the case of  $\alpha$ -ZrP.

The structural anomaly in  $\alpha$ -ZrP has very important implications in the intercalation chemistry reactions that these phosphates can undergo. Due to the layer expansion in the *ab* plane, the area per POH group (Table 2) is 24.0 Å<sup>2</sup> for  $\alpha$ -ZrP instead of the average value (21.50 Å<sup>2</sup>) for the other hydrogen phosphates. This means that for the intercalation of big guest species the availability of the active sites is higher in  $\alpha$ -ZrP. As a consequence of the higher free area, the charge surface density is lower for  $\alpha$ -ZrP.

Anisotropic Lorentzian peak broadening was found in the particular case of  $\alpha$ -SnP. This type of distortion originates from small particles with an anisotropic shape. Strain in the microparticles has been discarded since the peak broadening is better described by refining the Lorentzian Scherrer coefficient plus the anisotropic parameter. The microparticles are much longer in the *ab* plane than along the *c* axis. From the refined parameters we can estimate the particle size, resulting ca. 700 Å in the *ab* plane and ca. 100 Å along the *c*-axis.

Although our neutron powder diffraction study reveals that the hydrogen positions of the water molecule in  $\alpha$ -TiP are quite similar to those in  $\alpha$ -ZrP, we have not been able to determine the position of the hydrogens of the phosphate groups. This may be due to the fact that the H/D ratio in this case is close to 64% of H and 36% of D that would result in a 0 scattering factor (*b* lengths are  $-0.374$  and  $0.667$  for H and D, respectively). An alternative explanation may be that these hydrogen atoms are disordered. Anyway, we cannot confirm that the hydrogen-bond network in  $\alpha$ -TiP is only intralayer as in the  $\alpha$ -ZrP case.

The H positions are not known for  $\alpha$ -PbP, and only partially known for  $\alpha$ -TiP, but some insights about the forces that retain the hydration water molecule in this series of materials can be

obtained from the data given in Table 6. The narrow OH stretching vibration bands for gaseous water are centered at 3756 and 3657  $\text{cm}^{-1}$  for the asymmetric and symmetric stretchings, respectively.<sup>25</sup> It is well-known that interactions through H-bonds relax the O-H bond, which leads to a displacement of these bands to lower frequencies. In the studied materials, the water molecule interacts by an H-bond which displaces the positions of the asymmetric and symmetric stretching bands of the OH, which points to the free cavity, to  $\approx 3570 \text{ cm}^{-1}$  and  $\approx 3500 \text{ cm}^{-1}$ , respectively. But, a systematic trend in the variation of the frequencies in the series. For  $\alpha\text{-PbP}$ , the two OH stretching bands are centered at the lowest frequencies, which increase across  $\alpha\text{-TiP}$  and  $\alpha\text{-SnP}$ , being the highest values for  $\alpha\text{-ZrP}$ . Hence, it can be inferred that the hydration water molecule presents the strongest H-bonds in  $\alpha\text{-PbP}$ , while in  $\alpha\text{-ZrP}$  the water is the most weakly retained. This is in agreement with the TGA-DTA results that indicate that the water is lost at a quite low temperature ( $\approx 135 \text{ }^\circ\text{C}$ ) for  $\alpha\text{-ZrP}$ , at a much high temperature ( $\approx 200 \text{ }^\circ\text{C}$ ) in  $\alpha\text{-PbP}$ , and at intermediate values for  $\alpha\text{-SnP}$  and  $\alpha\text{-TiP}$ .

To refine these crystal structures at a better precision level and to determine the H-bond networks in these materials, we plan a combined powder X-ray and neutron diffraction study of fully deuterated highly crystalline  $\alpha\text{-TiP}$ ,  $\alpha\text{-ZrP}$ , and  $\alpha\text{-PbP}$ . This study will also clarify the forces that retain the hydration water molecule in the interlayer region of these materials.

---

(25) Nakamoto, K. *Infrared Spectra of Inorganic and Coordination Compounds*, 4th ed.; Wiley-Interscience: New York, 1986.

Finally, we point out that  $\alpha\text{-Pb}(\text{HPO}_4)_2 \cdot \text{H}_2\text{O}$  is one of the few salts of Pb(IV) structurally characterized. The average metal-oxygen bond distance is 2.11 Å, the  $\text{PbO}_6$  octahedra being quite distorted (see Table 2). This distortion of the octahedra may be an artifact due to the low precision in the positional parameters for the oxygen atoms. The combined X-ray and neutron study will give a more precise description of the structure.

### Conclusions

The syntheses of three  $\alpha\text{-M}(\text{HPO}_4)_2 \cdot \text{H}_2\text{O}$  compounds ( $\text{M} = \text{Ti, Sn, Pb}$ ) have been optimized to give single phases of highly crystalline materials. The crystal structures have been determined using the Rietveld method from X-ray powder diffraction data. These hydrogen phosphates are isomorphous and belong to the  $\alpha\text{-Zr}(\text{HPO}_4)_2 \cdot \text{H}_2\text{O}$  structure type. Although the prototype of this series is  $\alpha\text{-ZrP}$ , here we have shown that the volume of the unit cell of this compound is notably bigger than the volumes of the other members of the series. This is due to the presence of less corrugated layers in  $\alpha\text{-ZrP}$ . This anomaly has important implications in the intercalation chemistry of this phosphate compared with the other members of the series.

**Acknowledgment.** We are most grateful to Prof. Abraham Clearfield (Texas A&M University) for reading the manuscript and making helpful suggestions. This work was supported by CICYT research grants MAT-94-0678 and PB 93/1245. E.R.L. thanks the Junta de Andalucía (Spain) for a studentship.

IC940904J